

## Kink internal modes in discrete nonlinear chains

Fei Zhang

*Department of Computational Science, Faculty of Science, National University of Singapore, Singapore 119260*

(Received 20 May 1996)

We study localized modes around a kink in generalized Frenkel-Kontorova models with *anharmonic interparticle interactions*. We show numerically that such anharmonicity can give rise to *types of kink internal modes*, which oscillate with frequencies lying in the gaps either above or below the phonon frequency band. We analyze the kink internal modes with collective-coordinate approaches, and show that the low-frequency internal modes describe the kink shape (slope) fluctuations, whereas the highest-frequency internal modes are characterized by the out-of-phase oscillations of a few particles near the kink center. [S1063-651X(96)01810-7]

PACS number(s): 03.40.Kf, 63.20.Ry, 63.20.Pw

In recent years, the dynamics of *kinks* (topological solitons) has attracted considerable attention [1–12]. One important issue is to study the kinks' internal modes dynamics. Such internal modes include the kink translational mode and the kink internal shape modes. The former exists in all kink-bearing systems, while the latter exist only in some particular nonlinear Klein-Gordon models, including the  $\phi^4$  model and the double-sine-Gordon equation [1–4]. In particular, it has been found that the kink internal shape modes can contribute to the thermodynamic properties of the collective kink-phonon gas [1], and that they can cause unusual phenomenon (such as the resonances [2–4]) in the kink dynamics.

The previous studies [1–5] on the kink internal modes have been limited to cases where the interparticle interactions are harmonic. The main objective of the present paper is to investigate the kink internal modes in discrete chains with *anharmonic* nearest-neighbor interparticle interactions. Using the generalized Frenkel-Kontorova (FK) models as particular, but rather fundamental examples, we demonstrate that the kink can support not only a low-frequency (LF) internal shape mode but also one or several *high-frequency* (HF) internal modes due to the interplay between the discreteness and the anharmonicity in the interparticle interactions. In particular, we show that the LF kink internal shape mode (which oscillates with a frequency lying in the gap *below* the phonon frequency band) can exist for “soft” anharmonicity, whereas the HF kink internal modes (which oscillate with frequencies lying in the gap *above* the phonon frequency band) can exist for “hard” anharmonicity. These results can be understood with collective-coordinate approaches. We verify that similar results hold for many other kink-bearing systems with anharmonic interparticle interactions.

We begin our investigation with the generalized FK models that are defined by the (normalized) Lagrangian

$$\mathcal{L} = \sum_n \left\{ \frac{1}{2} \dot{\phi}_n^2 - W(\phi_{n+1} - \phi_n) - g^2 [1 - \cos(\phi_n)] \right\}, \quad (1)$$

where  $W(\cdot)$  is the nearest-neighbor interparticle interaction

$$W(x) = \frac{1}{2}x^2 + \frac{\alpha}{3}x^3 + \frac{\beta}{4}x^4, \quad (2)$$

$x = \phi_{n+1} - \phi_n$  being the relative displacement. In this model,  $\alpha$  and  $\beta$  are two parameters that control the strength of the anharmonicity; the parameter  $g$  determines the ratio of the substrate potential energy to the interparticle coupling energy and thus  $g$  is called the *discreteness parameter*. We note that many physical processes, including the spin dynamics in ferromagnetic systems [6], proton transport in hydrogen-bonded chains [7,8], planar rotations of the base pairs in DNA macromolecules [9], and polymer chain twistings [10,11], can be described by the FK-type models with strongly anharmonic interparticle interactions whose truncated Taylor series expansions are given by Eq.(2).

The equations of motion for the discrete chain can be written in the standard form

$$\ddot{\phi}_n - [W'(\phi_{n+1} - \phi_n) - W'(\phi_n - \phi_{n-1})] + g^2 \sin(\phi_n) = 0. \quad (3)$$

This system can support a kink solution which connects two equivalent ground states (e.g., 0 and  $2\pi$ ) of the substrate potential, provided that the parameters  $\alpha$  and  $\beta$  are positive, or greater than certain negative values [7].

In order to obtain the full spectrum of the linear excitations around the kink in the generalized FK model, we first use a direct numerical method. We look for a solution of Eq. (3) in the form

$$\phi_n(t) = \phi_n^K + \psi_n \exp(i\omega t), \quad (4)$$

where  $|\psi_n| \ll 1$ , and  $\phi_n^K$  represents the exact static kink solution of the systems. The kink is determined numerically by the following method: Starting with an approximate kink configuration given by the corresponding kink solution in the continuum limit, we use pseudomolecular dynamics with an artificial dissipation term to extract energy from the system until the chain is sufficiently relaxed [4]. The final kink profile is found to be always centered midway between two adjacent lattice sites. Throughout the paper, we consider a chain with a finite number of particles, i.e.,  $N=400$  or  $600$ , which is long enough to contain a kink. (The kink solution refers to the case where  $\phi_1^K = 0$  and  $\phi_N^K = 2\pi$ .)

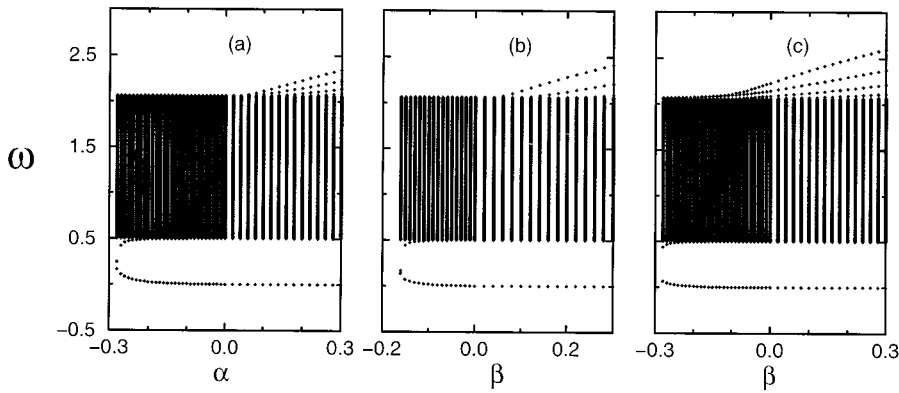


FIG. 1. The linear spectra of the generalized FK model in the presence of a kink. (a)  $g=0.5$ ,  $\beta=0$ ; (b)  $g=0.5$ ,  $\alpha=0$ ; (c)  $g=0.5$ ,  $\alpha=0.2$ .

Substituting the ansatz (4) into Eq.(3) and linearizing it with respect to  $\psi_n$ , we obtain a linear eigenvalue problem as follows:

$$M\Psi = \omega^2\Psi, \quad (5)$$

where  $\Psi = (\psi_1, \psi_2, \psi_3, \dots)^T$  is a column vector, and  $M$  is a symmetric tridiagonal matrix.

We have solved the eigenvalue problem (5) numerically for various sets of the model parameters  $\alpha, \beta$ , and  $g$  ( $0.2 < g < 1.0$ ). The (many) eigenfrequencies are presented in Fig. 1. The first feature to note is that there always exists an eigenfrequency (the lowest one), which is associated with the kink translational mode. This eigenfrequency is close to zero for  $\alpha > 0$  or  $\beta > 0$  (the hard anharmonicity), but it is shifted up for  $\alpha < 0$  or  $\beta < 0$  (the soft anharmonicity). In the latter case, the kink becomes narrower and feels a stronger discreteness effect.

Most interestingly, it is found that besides the lowest eigenfrequencies, there exist some other *isolated* eigenfrequencies outside the phonon frequency band [i.e., the interval  $(g, \sqrt{4+g^2})$ , as the many thick vertical lines in Fig. 1 have shown] when the anharmonicity is strong enough (depending on the discreteness parameter  $g$ ). In particular, from Fig. 1 we see that the soft anharmonicity can give rise to a kink internal shape mode [Fig. 2(a)] which oscillates with a frequency lying below the lower cutoff of the phonon frequency. On the other hand, the hard anharmonicity can give rise to one or several *high-frequency (HF) modes* localized around the kink. In particular, the highest-frequency mode is characterized by the out-of-phase oscillations of the neighboring particles [Fig. 2(b)].

In the case where both  $\alpha$  and  $\beta$  are nonzero and of opposite sign, it is their relative strength that will determine whether the LF or the HF kink internal modes can exist. For example, at  $g=0.5$  and  $\alpha=0.2$ , we find that if  $\beta$  is smaller than a critical value  $\beta_{c1} \approx -0.25$  the LF mode will appear; and if  $\beta$  is greater than  $\beta_{c2} \approx -0.19$  the HF modes will appear [see Fig. 1(c)]. For  $\beta$  in the interval  $(-0.25, -0.19)$  the kink has no internal modes except for the (trivial) translational mode, because the *hard* cubic and the *soft* quartic anharmonicity cancel out the effect of each other.

Given the results of the linear spectrum around a kink, the linear spectrum around an antikink can be easily obtained by using the symmetry of the model. For example, in the case

$\alpha \neq 0$  in which the kink-antikink symmetry is broken (see also Refs. [7,8]), the linear spectrum around an antikink is just the same as that around a kink *but* at the value of  $-\alpha$ .

To explain why the kink can support a LF internal shape mode, we use a simple collective-coordinate (CC) approach and we look for a solution of the form

$$\phi_n^L(t) \equiv \phi_n^L[Y(t)] = 4 \tan^{-1} \{ \exp[Y(n - n_0)] \}, \quad (6)$$

where  $Y(t)$  serves as a measure of the kink slope, and  $n_0$  represents the center-of-mass position of the stationary kink. We insert this ansatz into the system Lagrangian (1), and assume that the parameter  $g$  is so small that the PN potential can be neglected and that the sum over  $n$  can be replaced by the corresponding integral. After some computations we obtain the following effective Lagrangian

$$\mathcal{L}_e = \frac{\pi^2}{3Y^3} \dot{Y}^2 - U(Y), \quad (7)$$

where

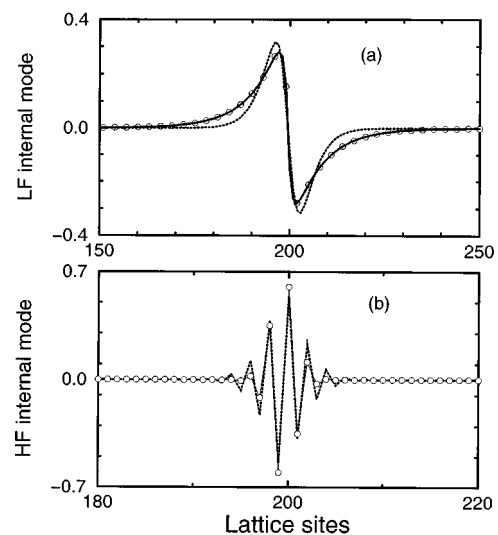


FIG. 2. (a) The normalized LF kink shape mode from the CC ansatz [see Eq. (14)] (dotted line), and from the direct numerical methods (circles), where  $g=0.42$ ,  $\alpha=0$ , and  $\beta=-0.2$ . (b) The normalized highest-frequency kink internal mode from the CC ansatz [see Eq.(16)] (dotted line), and from the direct numerical methods (circles), where  $g=0.8$ ,  $\alpha=0.0$ ,  $\beta=0.4$ .

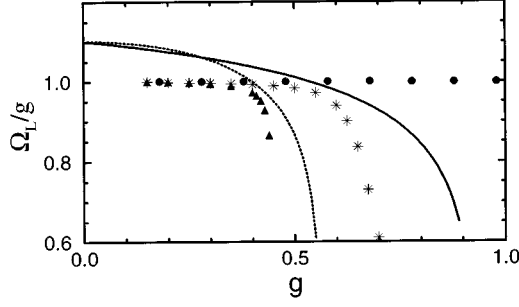


FIG. 3. The normalized frequency  $\Omega_L/g$  of the kink shape mode, as a function of the discreteness parameter. The solid (for  $\alpha = -0.2, \beta = 0$ ) and the dotted ( $\alpha = 0, \beta = -0.2$ ) curves are the CC results Eq. (12). The stars ( $\alpha = -0.2, \beta = 0$ ), the triangles ( $\alpha = 0, \beta = -0.2$ ), and the circles ( $\alpha = 0, \beta = 0$ , for the standard FK model), are from the direct numerical calculations.

$$U(Y) = 4Y + \frac{4}{3}\alpha\pi Y^2 + \frac{16}{3}\beta Y^3 + 4g^2/Y. \quad (8)$$

The equation of motion for the collective variable is

$$\frac{2\pi^2}{3Y^3}(\ddot{Y} - 3\dot{Y}^2/Y) + \frac{\partial U}{\partial Y} = 0, \quad (9)$$

which is useful for analyzing the kink slope fluctuation. First, we note that the equilibrium kink slope should satisfy  $(\partial U/\partial Y) = 0$ , or

$$Y^2 + \frac{2\pi}{3}\alpha Y^3 + 4\beta Y^4 = g^2, \quad (10)$$

from which the equilibrium kink slope  $Y = Y_0$  can be obtained as a function of the discreteness parameter  $g$  and the anharmonic parameters  $\alpha$  and  $\beta$ .

The small-amplitude fluctuations of the kink slope around its equilibrium  $Y_0$  can be analyzed by substituting  $Y(t) = Y_0 + y(t)$ , where  $Y_0 = Y_0(\alpha, \beta, g)$  is the solution of  $Y$  from Eq. (10) and  $|y(t)| \ll 1$ , into Eq. (9). We linearize the equation with respect to  $y(t)$  to obtain

$$\frac{2\pi^2}{3Y_0^3}\ddot{y} + \left[ \frac{\partial^2 U}{\partial Y^2}(Y_0) \right] y = 0. \quad (11)$$

Therefore, the kink slope fluctuates with the frequency

$$\Omega_L = \left[ \frac{3Y_0^3}{2\pi^2} \frac{\partial^2 U}{\partial Y^2}(Y_0) \right]^{1/2} = \frac{2\sqrt{3}}{\pi} g \left( 1 + \frac{\alpha\pi Y_0^3}{3g^2} + \frac{4\beta Y_0^4}{g^2} \right)^{1/2}, \quad (12)$$

which depends strongly on the three parameters  $\alpha$ ,  $\beta$ , and  $g$ . In particular, we have checked that for a given value of  $g$ ,  $\Omega_L$  can become smaller than the lower cutoff of the phonon frequency  $g$ , if  $\alpha$  or  $\beta$  takes a suitably large *negative* value. This agrees well qualitatively with the numerical results shown in Fig. 1

In Fig. 3 we plot the normalized frequency  $\Omega_L/g$  against  $g$  (for the given sets of  $\alpha$  and  $\beta$ ) and compare it with the direct numerical results. It is seen that in the continuum regime where  $g \ll 1$ , the kink has no low-frequency shape modes. This is consistent with the fact that, when  $g \ll 1$ , Eq.

(3) can be well approximated by the sine-Gordon (SG) equation in which the kink has no internal shape modes. However, in the weak discrete regimes where  $g$  is not so small, we observe that  $\Omega_L$  actually lies in the gap below the phonon frequency band, displaying qualitative agreement with the direct numerical results. Noting that the kink in the standard FK model has no true internal shape modes for a wide range of discreteness parameter (Fig. 3), we conclude that the existence of the kink internal shape mode in the generalized FK models is due to the interplay between the anharmonicity and the discreteness effect.

Since the CC approach amounts to using a one-parameter ansatz (6) to approximate the kink (and its shape mode) solution (4), which has many degrees of freedom, it might not be quantitatively accurate, as indicated in Fig. 3. On the other hand, the fluctuating kink obtained through the CC approach [cf. Eqs. (6), (11)] is

$$\phi_n^L = 4 \tan^{-1} \{ \exp[(Y_0 + y(t))(n - n_0)] \} \approx \phi_n^s + y(t) \psi_n^L, \quad (13)$$

where  $\phi_n^s = 4 \tan^{-1} \{ \exp[Y_0(n - n_0)] \}$ , and

$$\psi_n^L = \frac{2(n - n_0)}{\cosh[Y_0(n - n_0)]}. \quad (14)$$

Therefore, the function  $\psi_n^L$  can be considered as an approximation to the kink shape mode. We find that in the weak discrete regime,  $\psi_n^L$  can describe the kink internal shape mode reasonably well [Fig. 2(a)].

In order to understand why the HF kink internal modes can appear, we notice that the mode associated with the highest eigenfrequency is characterized by the out-of-phase oscillations of neighboring particles, and that the amplitude of the mode decays rapidly away from the kink center [Fig. 2(b)]. This prompts us to use the ansatz,

$$\phi_n^H(t) = 4 \tan^{-1} \{ \exp[Y_0(n - n_0)] \} + A(t) \psi_n^H, \quad (15)$$

where  $Y_0$  is the kink's equilibrium slope determined from Eq. (10),  $|A(t)| \ll 1$ , and

$$\psi_n^H = \frac{(-1)^n \sqrt{Y_0}}{\sqrt{2} \cosh[Y_0(n - n_0)]}, \quad (16)$$

is used to approximate the highest-frequency kink internal mode.

Again we substitute the ansatz (15) into the system Lagrangian and compute the effective Lagrangian to obtain (all the constant terms are dropped)

$$L_e = \frac{1}{2} \dot{A}^2 - \frac{1}{2} (4 + 4\alpha\pi Y_0 + 32\beta Y_0^2 - \frac{2}{3}g^2) A^2. \quad (17)$$

Therefore, the frequency of the dynamical variable  $A(t)$  is

$$\Omega_H = \sqrt{4 + 4\alpha\pi Y_0 + 32\beta Y_0^2 - (2/3)g^2}, \quad (18)$$

which, like Eq. (12), depends strongly on the model parameters. In particular, for a fixed discreteness parameter  $g$ ,  $\Omega_H$  can become greater than the highest phonon frequency  $\omega_{max} = \sqrt{4 + g^2}$  if  $\alpha$  or  $\beta$  takes a large *positive* value.

In Fig. 4 we plot the normalized frequency  $\Omega_H/\omega_{max}$  as a

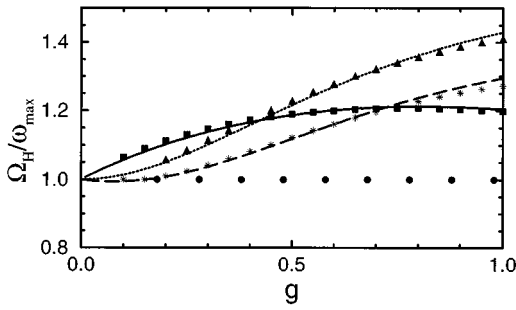


FIG. 4. The normalized frequency  $\Omega_H/\Omega_{\max}$  of the highest-frequency kink internal mode, as a function of the discreteness parameter. The solid (for  $\alpha=0.4, \beta=0$ ), the dotted ( $\alpha=0, \beta=0.4$ ), and the long-dashed ( $\alpha=-0.1, \beta=0.3$ ) curves are the CC results [Eq. (18)] which are in good agreement with the corresponding numerical results (symbols). The circles are the numerical results for the standard FK model.

function of  $g$  for various sets of the anharmonic parameters. It turns out that the analytical results are in very good agreement with the exact numerical ones. This is a consequence of the fact that the function  $\psi_n^H$  is a good approximation to the true highest-frequency kink internal mode [Fig. 2(b)]. We also note that the kink in the standard FK model ( $\alpha=0, \beta=0$ ) cannot support high-frequency internal modes due to the absence of anharmonicity in the interparticle interactions.

For certain ranges of the model parameters the kink may have more than one HF internal mode. However, it seems difficult to describe the other HF modes by simple CC methods, because their patterns are much more complex than that of the highest-frequency mode.

In order to check the generality of the present results, we have carried out numerical calculations for several other discrete kink-bearing systems with anharmonic interparticle interactions, including the FK-type models with the sinusoidal interparticle interaction,  $W(x)=[1-\cos(x)]$  [9], or the Toda interaction,  $W(x)=(1/A^2)[\exp(-Ax)-1+Ax]$ . We have found that for certain ranges of the model parameters the kink can support a LF internal shape mode. This is because the Taylor series of each of the two functions  $W(x)$  has a soft anharmonic term. In addition, we have also examined a generalized  $\phi^4$  model with the anharmonic interparticle couplings (2). In this case, the oscillation frequency of the kink internal shape mode, which already exists in the standard  $\phi^4$  model [2], can be shifted due to the effects of the anharmonicity. Moreover, the hard anharmonicity can give rise to HF kink internal modes, just as what is shown in the generalized FK model.

In conclusion, we have demonstrated that the anharmonicity in the interparticle interactions together with the weak discreteness effect can allow the kink to support either low-frequency or high-frequency internal modes, depending on the nature of the anharmonicity. We have described the low-frequency kink shape mode and the highest-frequency kink internal mode with the collective-coordinate methods. It should be remarked that, while the LF kink internal modes can also exist in continuum models, the HF kink internal modes can only exist in discrete systems, whose phonon frequency has an upper bound. It remains to be investigated how the kink dynamics in the discrete nonlinear chains can be influenced by both the LF and the HF internal modes discussed in the present paper.

This work is supported by the Academic Research Grant (No. RP950601) at the National University of Singapore.

- 
- [1] J.F. Currie, J.A. Krumhansl, A.R. Bishop, and S.E. Trullinger, Phys. Rev. B **22**, 477 (1980); R. Giachetti, P. Sodano, E. Sorace, and V. Tognetti, *ibid.* **30**, 4014 (1984).
- [2] D. K. Campbell, J.F. Schonfeld, and C.A. Wingate, Physica D **9**, 1 (1983); M. Peyrard and D.K. Campbell, *ibid.* **9**, 33 (1983); D. K. Campbell, M. Peyrard, and P. Sodano, *ibid.* **19**, 165 (1986).
- [3] F. Zhang, Yu.S. Kivshar, and L. Vázquez, Phys. Rev E **46**, 5214 (1992).
- [4] P.T. Dinda and C.A. Willis, Physica D **70**, 217 (1993); Phys. Rev. E **51**, 4958 (1995).
- [5] J.A. Holyst and H. Benner, Phys. Rev. B **52**, 6424 (1995).
- [6] H.J. Mikeska, J. Phys. C **11**, L27 (1978).
- [7] O.M. Braun, F. Zhang, Yu.S. Kivshar, and L. Vázquez, Phys. Lett. A **157**, 241 (1991).
- [8] Y.P. Mei, J.R. Yan, X.H. Yan, and J.Q. You, Phys. Rev. B **48**, 577 (1993).
- [9] S. Takeno and S. Homma, J. Phys. Soc. Jpn. **55**, 65 (1986); **55**, 2547 (1986).
- [10] F. Fillaux and C.J. Carlile, Phys. Rev. B **42**, 5990 (1990); F. Fillaux, C.J. Carlile, and G.J. Kearley, *ibid.* **44**, 12 280 (1991).
- [11] F. Zhang, M.A. Collins, and Yu. S. Kivshar, Phys. Rev. E **51**, 3774 (1995).
- [12] R. Boesch and C.R. Willis, Phys. Rev. B **42**, 2290 (1990); M.J. Rice, *ibid.* **28**, 3587 (1983).